CHAPTER 4

Application of Electro-Optic Materials: Design of Polymeric Optical Modulators

---

4.1. Introduction

In recent years, electro-optic polymers have been used to make various optical devices in the telecommunication field due to several advantages. They demonstrate some advantages over traditional optical materials, and they can be used to produce high performance, low cost devices, such as electro-optic modulators, variable optical attenuator (VOA), and tunable filter.

Polymeric optical devices can be made from a thin film multilayer structure comprising a substrate (glass, silicon, etc.), a lower electrode (silver, gold, etc.), a lower polymer cladding, a central wave-guide layer made of the polymer exhibiting a larger refractive index than those of the cladding layers, an upper cladding layer, and a second electrode. A schematic picture of such a device is given in Figure 4-1[(1)].

The polymer layers, deposited by ESA, spin coating or cast dipping, have thicknesses on the order of microns or even less, depending upon whether mono-mode or multimode wave-guides are desired, and the operation frequency. Thickness homogenetities of better than 1% over 3 inch diameter silicon wafer areas have been

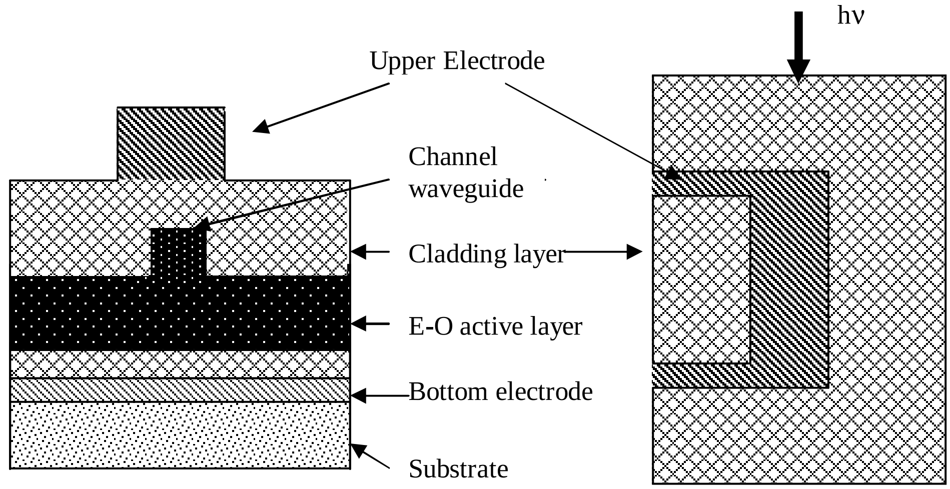

Fig. 4-1. Schematic of channel waveguide structure (left) and top view of wave-guide multilayer (right).

achieved by spin coating. The electrode thicknesses range from100 nm to100 μm, depending on the electrical driving system and the type of electrodes. The electrode has two functions: first, to allow a means for electric field poling to induce E-O behavior in the core material; second, to apply switching voltages to the produced devices. Poling is produced by placing the multilayered material in an oven at a temperature slightly below the Tg of the material and at an electric field strength excess of 20 V/micron.

Several techniques are used in device fabrication and are described below.

Photobleaching This technique has been developed to pattern devices such as electro-optic switches. The refractive index of a completely bleached film can be decreased isotropically by 3×10^{-2}. The exposure time needed for a complete bleaching of the film depends on its thickness. Following this method, single mode ridge wave-guides have been processed by exposing a film using a common geometrical mask.

Selective poling In this method, when an electro-optic polymer is poled, the film becomes birefringent. If n is the refractive index of the unpoled material, after orientation, the layer will exhibit an extraordinary index n_e in the direction parallel to the poling field and an ordinary index n_o in the direction perpendicular to the poling field vector, satisfying $n<n_o<n_e$. The poling voltage may be applied on electrodes patterned so as to define the waveguide geometry. The primary advantage of this method is that both poling and waveguide fabrication processes are achieved in one step, although such waveguides are polarization-selective, a disadvantage which may limit the area of their application. The index change induced by poling depends on the nature of the electro-optic polymer and on the magnitude of the applied electric poling field.

Strip loaded wave-guide This type of waveguide is formed by the patterning of a high index strip on top of or below an active guiding layer. Such a geometry can be achieved either by local ion exchange approaches or by the PECVD deposition of a high index dielectric strip.

Channel wave-guide Increasing the thickness of the guiding layer can be achieved either by defining an inverted ridge in the bottom buffer layer by using a UV curable resin by reactive ion etching, or by etching grooves in the silicon substrate. Another way to fabricate such a two dimensional waveguide is to burn a strip of high index core material into a lower index cladding polymer.

Based on the above discussion, it is clear that for high performance modulators, electro-optic materials with high electro-optic coefficient, low dielectric coefficient, low optical absorption coefficient, a high degree of homogeneity, and high thermal and optical stability are highly desirous.

Lithium niobate is currently the dominant material in modern electro-optic modulators. It is a crystalline ferroelectric material. Commercial lithium niobate modulators are now available from companies such as Lucent, Corning and Agilent Technologies. They have bandwidths of about 10-70 GHz with V_π of 5-6 V and very low insertion loss (0.5-5 dB). But polymer based modulators have many potential advantages over lithium niobate modulators. Polymeric modulators can achieve very high bandwidths, due to the near equality of the refractive index n at optical and millimeter wavelengths, so that optical and millimeter wave electromagnetic radiation can co-propagate over significant distance without de-phasing. Carefully designed lithium niobate modulators with clever velocity matched (traveling wave) structures have been demonstrated at 70 GHz, but a simple structured polymeric modulator can operate at a bandwidth of 100-200 GHz, and a 3dB bandwidth of 361 GHz has been demonstrated [(2)]. EO polymers have low relative permittivity, allowing the positioning of several individual high speed modulators close to each other without significant cross-talk between the individual modulators. This means that high density packaging and integration with very large scale integration (VLSI) semiconductor electronics is possible. EO polymers are also compatible with a variety of materials. This is a significant feature, for it allows the possibility of making integrated optical-chips, and the integration of EO polymers with other optic materials, Finally, the application of EO polymers creates the potential for dramatically lower operation voltage. Driving voltages of less than 1 volt have been demonstrated. Compared with the driving voltage of 5-6 volts for lithium niobate modulators, this represents significant progress.

In this chapter, some basic aspects of polymeric devices will be discussed. Although they will mainly be focused on electro-optic modulator waveguide structure and sizes, these conclusions are also useful for other waveguide devices.

4.2. Waveguide analyses by means of effective index approach

4.2.1. Minimum (cut off) thickness of planar waveguide

This section describes the electromagnetic field confinement effect in planar waveguide structures.

Starting from the electromagnetic wave function for electric field components

$$\nabla^2\mathbf{E} + k^2n^2\mathbf{E} = 0, \tag{4.1}$$

where n is the refractive index, $k = 2\pi/\lambda$, k is the wave number, and λ is the wavelength. Assuming wave propagation along z direction,

$$E = \exp[i(\omega t-\beta z)], \tag{4.2}$$

where ω is the optical frequency, and β = nk is the wave propagation constant. Also assuming no field variation in the y direction, the wave equation (4.1) in each region then becomes

$$\frac{d^2E}{dx^2} + (k^2n_i^2 - \beta^2)E = 0\,, \tag{4.3}$$

where n_i is the refractive index of the i^{th} region, typically termed the effective refractive index, which can be defined as

$$n_e = \frac{\beta}{k}. \tag{4.4}$$

Applying the wave function to wave propagation in each region (region 1~3) for this planar waveguide case, as illustrated in Figure 4-2, light is confined in region 2 (i.e. as a bound mode) only when

$$n_3 < n_{e,2} < n_2. \tag{4.5}$$

Now assuming $n_3 \geq n_1$, it can be found that n_e increases with t, and at certain thickness of layer 2, n_e approaches n_3, and light is no longer confined in region 2. This defines the critical cutoff thickness(3) as

$$t_{cutoff,m} = \frac{\lambda}{2\pi(n_2^2 - n_3^2)^{1/2}}\left(m\pi + \tan^{-1}\frac{\zeta_1(n_3^2 - n_1^2)^{1/2}}{\zeta_2(n_2^2 - n_3^2)^{1/2}}\right), \tag{4.6}$$

where $\zeta_i = 1$ for TE mode (transverse electric mode, having its electric field component parallel to the plane of the interfaces between the regions), $\zeta_i = 1/n_i^2$ for TM mode (transverse magnetic mode, having its electric field component perpendicular to the interfaces), and m is the mode number. The mode number is the number of solutions of the wave equation. For singlemode (basic made) operation, m = 0. In general, for m>0, the number of modes supported by a waveguide is approximately given by

$$M = \frac{2T}{\lambda}(n_2^2 - n_1^2)^{1/2}. \tag{4.7}$$

Figures 4-3 and 4-4 are the dispersion curve and high frequency (optical) relative dielectric constants of ESA PS-119 and CdSe films respectively. Relative dielectric constants can be calculated by equation $\varepsilon_r^{1/2} = n + ik$, or $\varepsilon_r = n^2 - k^2$, n and k are refractive index and extinction ratio respectively in figure 4-3. From these figures, the refractive index of ESA PS-119 and CdSe nano-cluster based films is seen to decrease slowly with increasing wavelength, and they tend to be constant at longer wavelengths, specifically 1.51 for PS-119 polymer film, and 1.61 for CdSe films(when wavelength >1100 nm), respectively. They are a little higher than silica glass' refractive index (~1.50), but lower than semiconductor's refractive index (>2), so semiconductor wafers (such as Si, GaAs, InP) are not suitable for substrates, but silica glass is ideal for substrate in device fabrication, in part because the refractive index of glass can be adjusted easily by changing its composition. For typical homogeneous and transparent polymer films, the refractive index is related to the light wavelength or frequency in terms of Cauchy model, given as

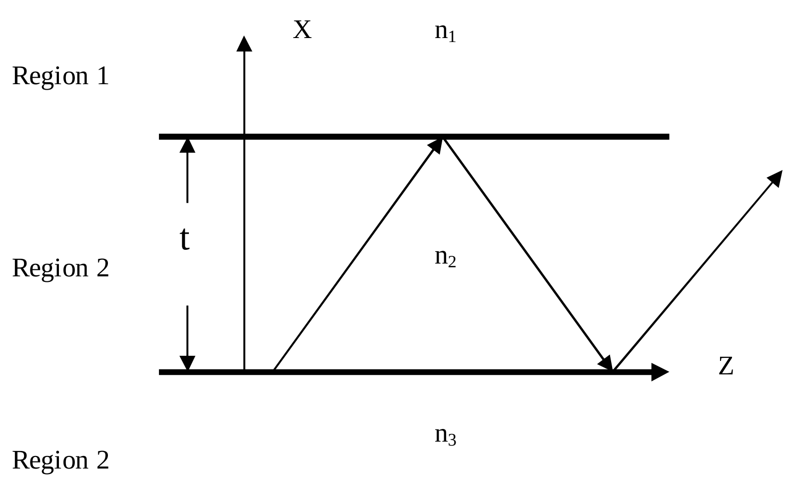

Fig. 4-2. Configuration of planar waveguide.

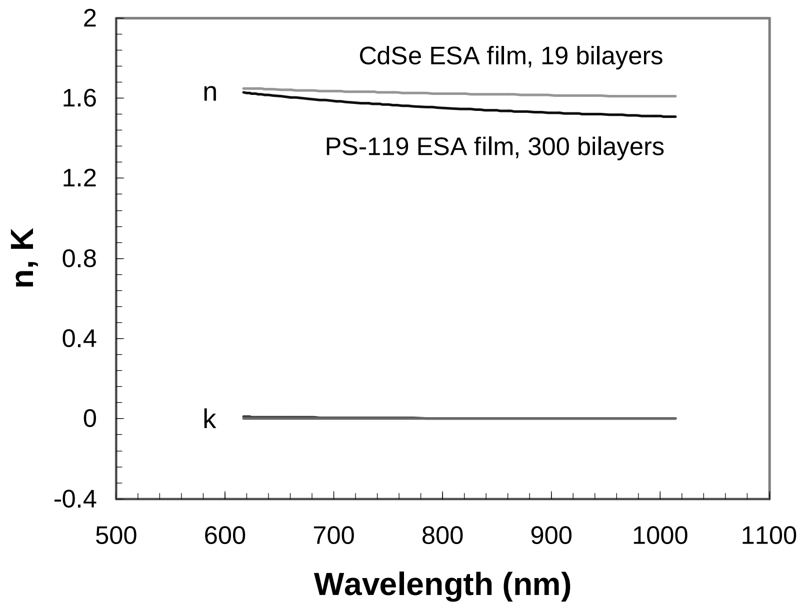

Fig. 4-3. Dispersion curve of ESA PS-119 and CdSe films.

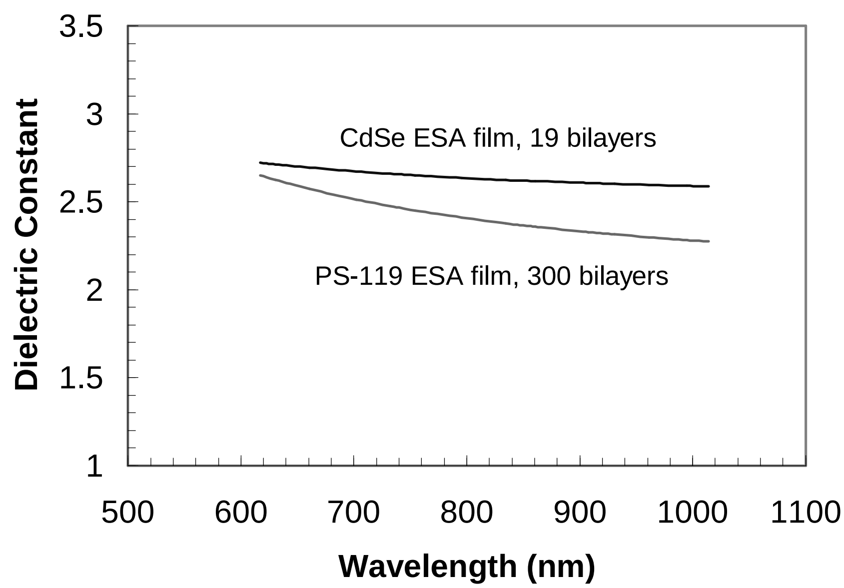

Fig. 4-4. High frequency (optical) dielectric constant of ESA PS-119 and CdSe films.

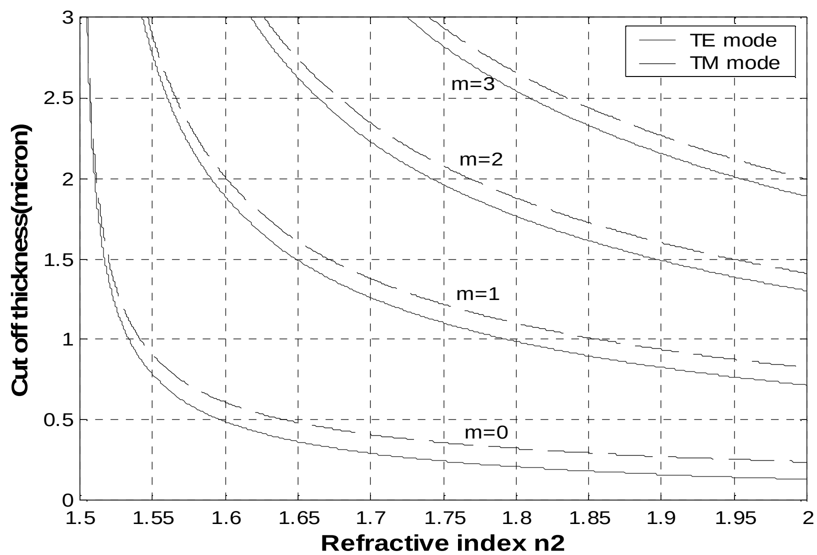

Fig. 4-5. Cutoff thickness of plane waveguide variation with refractive index of core

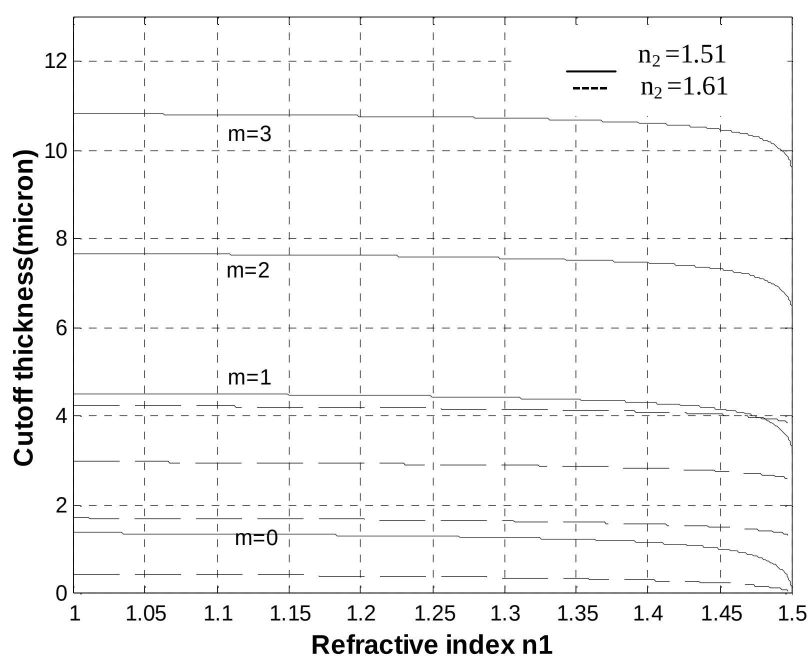

Fig. 4-6. Cutoff thickness of plane waveguide variation with refractive index of cladding layer, n_2=1.51 and 1.61, n_3=1.50, wavelength=1550nm.

$$n(\lambda) = n_1 + \frac{n_2}{\lambda^2} + \frac{n_3}{\lambda^4}, \tag{4-8}$$

where n_1, n_2, n_3 are Cauchy numbers[(4)].

Figures 4-5 and 4-6 are calculated results of cutoff thickness for thin film waveguides. From these results, it is clear that lower modes require lower cutoff thickness than higher modes, and that for the same mode, the TE mode has lower cutoff thickness. It is also apparent that the higher the core layer refractive index, the lower the cutoff thickness. Thus, so for single mode (m=0) TE mode operation, the cutoff thickness is 2.5 micron for polymer films (n_2=1.51), and is 0.4 micron for CdSe films (n_2=1.61). These thicknesses define the minimum film thickness required for waveguide, below which no light wave can propagate through films, and above which films may support more than one mode. Cutoff thickness is affected more by n_2 than by n_1, although it changes slightly with n_1.

4.2.2. 3-D Channel (ridge) waveguide

Most waveguide devices consist of single mode 3-D channel waveguides to attain highly efficient control of the guided mode. Figure 4-7 shows the structure of a 3-D channel waveguide. There are a cladding layer, a core layer, and a substrate, with refractive indices of n_1, n_2 , and n_3, respectively. For the case that $n_2 > n_3 > n_1$, the light is confined in the core layer, in which the propagation constant β along the z direction exists in the range of $k_0 n_3 < \beta < k_0 n_1$, where $k_0 = 2\pi/\lambda$, λ is the wavelength, $\beta = k_0 n_e$, n_e is the effective index, and $n_3 < n_e > n_1$. A 3-D waveguide can be divided into two 2-D

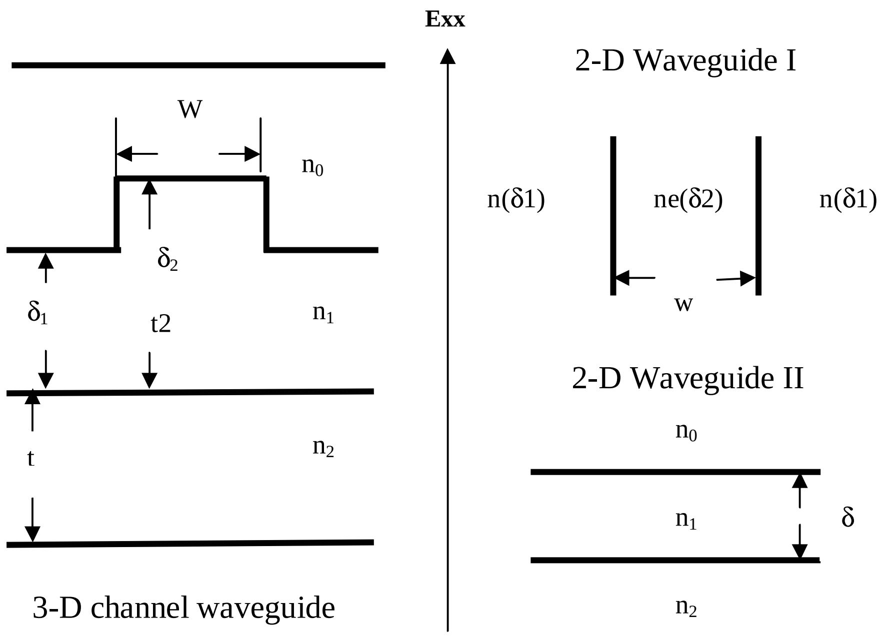

Fig. 4-7. Configuration of 3-D channel waveguide.

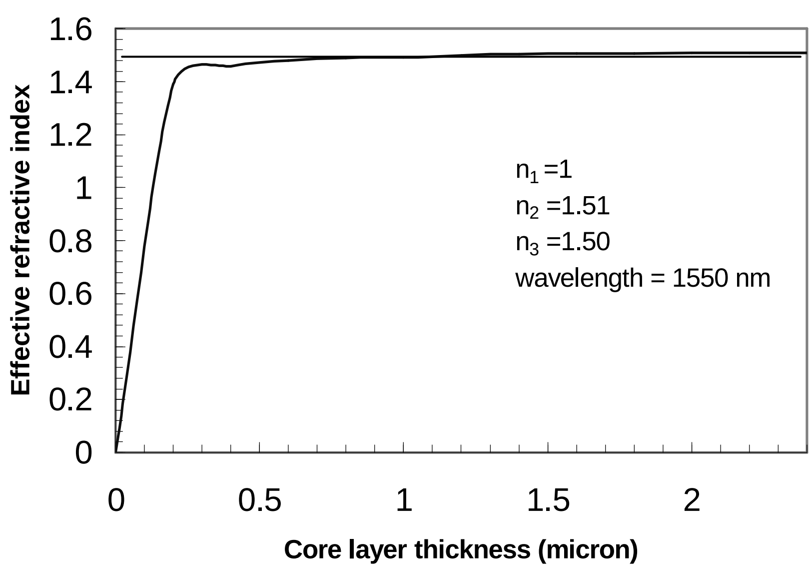

Fig. 4-8. Effective refractive index versus core layer thickness.

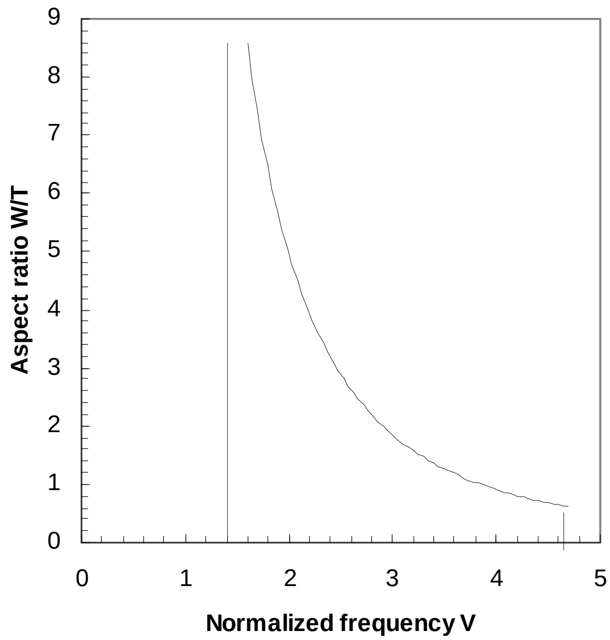

Fig. 4-9. Aspect ratio as a function of normalized frequency of 3-D channel waveguide.

waveguides, as depicted in Figure 4-7. Here, 2-D waveguide I (with thickness = t) can be described by the dispersion equation of the TE mode(5)

$$V\sqrt{1-b} = (m+1)\pi - \tan^{-1}\sqrt{\frac{1-b}{b}} - \tan^{-1}\sqrt{\frac{1-b}{a+b}}\,, \tag{4.9}$$

where V is the normalized frequency, b is the normalized guide index, and a is the asymmetric parameter. These can be expressed as

$$V = kt\sqrt{n_2^2 - n_3^2}\,, \tag{4.10}$$

$$b = \frac{n_e^2 - n_3^2}{n_2^2 - n_3^2}, \text{ and} \tag{4.11}$$

$$a = \frac{n_3^2 - n_1^2}{n_2^2 - n_3^2}. \tag{4.12}$$

n_e can be determined by these equations, and the result is shown in Figure 4-8. It can be seen that the effective refractive index $n_e \leq n_2$. When the thickness is larger than 1.5 microns, n_e is close to n_2, and when $n_e = n_3$, the corresponding thickness is the cutoff thickness, which is close to the results shown in Figures 4-5 and 4-6.

Another 2-D waveguide (waveguide II with thickness = w, perpendicular to waveguide I) can be also described by the above dispersion equation, just by replacing thickness t by width w in equation (4.10).

Combining the dispersion equation in these two cases, we obtain the relation between the aspect ratio W/T and normalized frequency V, and the result is shown in Figure 4-9. In practice, waveguide devices require single mode waveguides in which light is as strongly confined as possible to reduce loss. For this reason, the aspect ratio and normalized frequency should be close to the upper part of the geometrically closed area shown in Figure 4-9. This is an important design guideline for channel waveguides. For our electro-optic polymer ESA film (n=1.51) and CdSe ESA film (n=1.61), if the wavelength is 1550 nm, n_3 =1.50, t=3000 nm (polymer ESA film) and 1500 nm (CdSe ESA film), then V= 2.11 for the polymer ESA film and 3.55 for the CdSe ESA film. Thus, W/T = 4.1 for the polymer ESA film and 1.1 for the CdSe ESA film, and w = 12.3 microns for the polymer ESA film and 1.65 microns for the CdSe ESA film.

4.3. High speed operation and traveling wave electrode design

4.3.1. High speed device

In order to have devices that operate at high frequencies effectively, some basic factors limiting the highest operation frequencies and it should be addressed, as summarized here.

Rise-time budget The purpose of the rise-time budget is to ensure that the system is able to operate properly at the intended bit rate. The total rise time of the entire system is related to the individual component rise times approximately by [6]

$$T_r^2 = T_{tr}^2 + T_{fib}^2 + T_{rec}^2, \tag{4.13}$$

where T_{tr} , T_{fib} , T_{rec} are the individual rise times of the transmitter, optical fiber channel, and receiver, respectively. These are determined by materials rise time and electrical circuit rise time (= 2.2 RC) effects. It is common to use $T_r\Delta f$ =0.35 in the design of optical communication systems as a conservative guideline. So, if the bandwidth is 100GHz, the rise time should be 3.5 ps. Figure 4-10 (a) and (b) show the ultrafast laser pulse response of CdSe nano-cluster doped glass measured under different pulse intensity conditions of the pumping beam. The rise time is less than 1 ps and varies slightly with pulse intensity.

Currently, inorganic electro-optic crystals are predominately used in optical devices, and their material rise time limits the operation bandwidth of devices to less than 100 GHz. For next generation high speed communications and networks (particularly in the

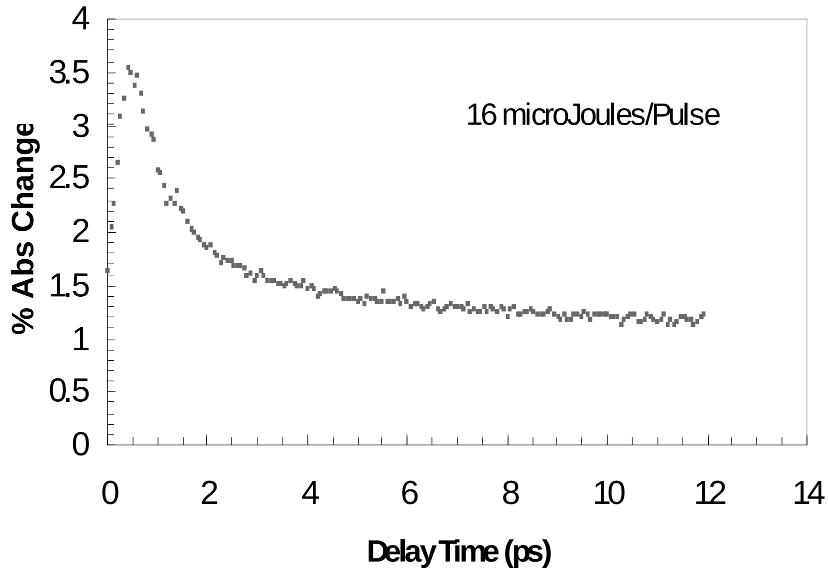

(a) 16 Microjoules/pulse

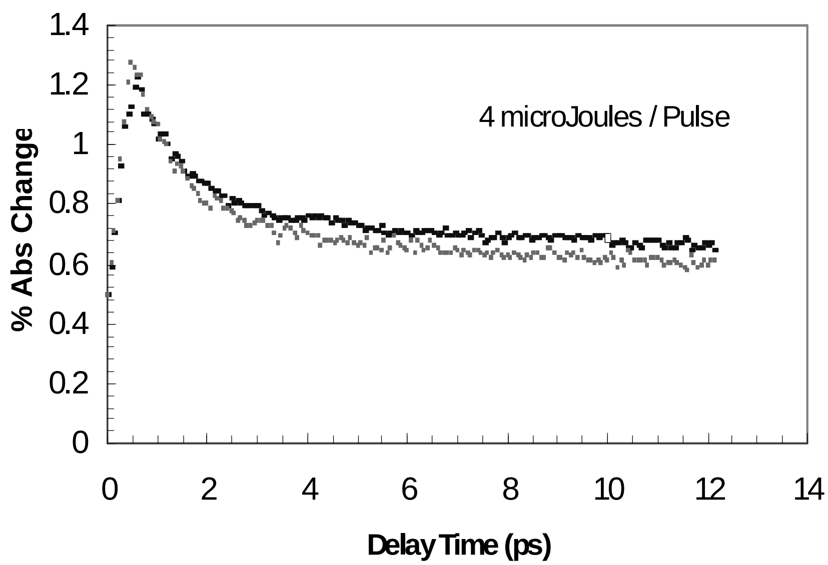

(b) 4 Microjoules/pulse

Fig. 4-10. Ultrafast laser spectroscopy of CdSe nano-cluster doped glass at different pulse intensities.

long haul market), new materials have to be developed and adopted.

Material limitation A modulator can be considered as a electro-optic material placed between two electrodes, in a geometry similar to that of a parallel plate capacitor, with an internal resistance R_s, load resistance R_l, and capacitance C. It is electrically equivalent to an RLC resonant circuit. Since $R_l > R_s$ so most of the modulation voltage appears across the electro-optic material. The simplified equivalent circuit has a finite resonant frequency over a frequency interval (modulation band width) $\Delta\omega$[7] given by

$$\frac{\Delta\omega}{2\pi} = \frac{1}{2\pi R_L C}. \tag{4.14}$$

From (4.14), it is obvious that low R_L and C are good for high bandwidth. Electro-optic materials with low dielectric constants are prefered for high speed optical devices. Specifically, electro-optic polymers that possess lower dielectric constants (<3) than their inorganic crystal partners (>3) are advantageous. This is one important reason to choose electro-optic polymers for use in high speed device materials.

Transit time limitation Because of the birefringent nature of electro-optic materials, when a beam propagates through them along certain direction other than their optic (z) axis, two components of the beam (the o component and the e component) experience different path lengths, so there is a phase difference between the two components at a physical distance l; this is electro-optic retardation. Retardation is proportional to $\frac{1-e^{i\omega_m\tau_d}}{\omega_m\tau_d}$, where ω_m is the modulation frequency, and $\tau_d = nl/c$ is the transit time. When $\omega_m\tau_d = \pi/2$, $\frac{1-e^{i\omega_m\tau_d}}{\omega_m\tau_d}$ =0.9; this defines the highest useful modulation frequency $(\nu_m)_{\max} = \frac{c}{4nl}$.

The highest useful modulation frequency decreases with increasing L. In this respect, lengthy modulation due to any effect is not desired. Similarly, if the electric and optic refractive indexes of electrodes and waveguide are different, electric field and optic field propagate at different speed. This causes another transit time limitation. In order to overcome the transit time limitation, the electric field and the optical field should propagate at the same speed. This can be achieved by means of traveling-wave configuration of electrodes and modulators, which can be implemented by carefully designing the shape, size, and properties of the electrodes and modulator waveguide.

Modulation efficiency can be described by modulation index δ

$$\delta = \beta L \frac{\sin \frac{\omega_m}{2c}(n_m - n)L}{\frac{\omega_m}{2c}(n_m - n)L}, \tag{4.15}$$

where β is the propagation parameter and L is the modulation length. The output amplitude of the modulator is proportional to exp(iδ). However, the modulation index is then not proportional to L, as is illustrated in Figures 4-11 and 4-12. By analysis, the maximum modulation index can be reached at

$$L = \frac{\pi C}{\omega_m |n_m - n|}, \tag{4.16}$$

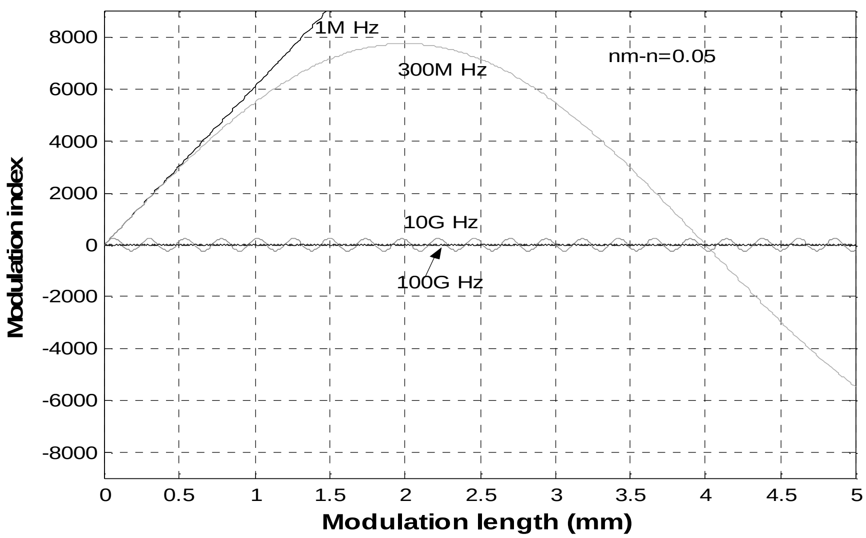

Fig. 4-11. Modulation index as a function of modulation length at different modulation frequency, n=1.51, n_m =1.56.

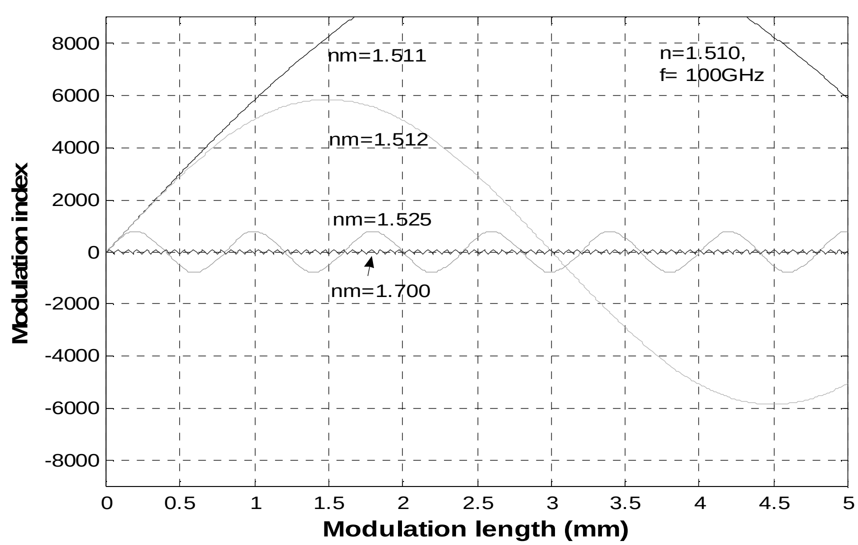

Fig. 4-12. Modulation index as a function of modulation length at different n_m, n=1.51, ω_m =100G Hz.

L verses n_m can be plotted to which determine the optimum length of the modulator.

These Two figures provide design guidance. From these figures, you be seen how the modulation index is affected by modulation frequency, and how modulation index decreases sharply at high modulation frequency. It is clear that only for low refractive index differences ($\Delta n=n_m-n$) and modulation frequencies, the modulation index always increases with length linearly. At high refractive index difference and modulation frequency, the modulation index reaches a maximum value periodically, so increasing the modulation length cannot ensure to an increase in the modulation index. It is also clear from these figures that higher Δn and modulation frequency lead to lower modulation index. This is particularly important at high modulation speeds, because proper modulation length should be determined based on the refractive index and modulation frequency. For example, when $\Delta n=n_m-n = 0.05$ and modulation frequency = 0.3GHz, the optimal modulation length should be around 2n times 2.1 mm (n is integral), or, when the modulation frequency = 100GHz, for a reasonably high modulation index, $\Delta n=n_m-n <0.002$, Thus, control of both n_m and n is very important to achieve high speed operation, and this is a nontrivial problem.

In determining length L, two other factors should be also considered. One is bandwidth; the other one is half-wave voltage. Increasing L will increase the effective overlap integration distance, so the half-wave voltage can be reduced. However, this will led to the reduction of bandwidth (see chapter one), so in practice, there is trade off between bandwidth and half-wave voltage. As a result, L is typically several millimeters to several centimeters.

4.3.2. Traveling wave electrode design

Traveling wave operation is shown in Figure 4-13. While the optical wave travels through optical waveguide, the microwave travels through the electrode, If the traveling wave configuration is implemented, the optical wave and the microwave have the same propagation speeds, so both are spatially in phase, and maximum modulation thus is reached. This requires the values of optical refractive index and microwave refractive index to be the same, or very close, or the modulation efficiency (in terms of modulation index) to be low. For traveling wave electrode modulators, the factors limiting the performance of the modulator are known to be the following.

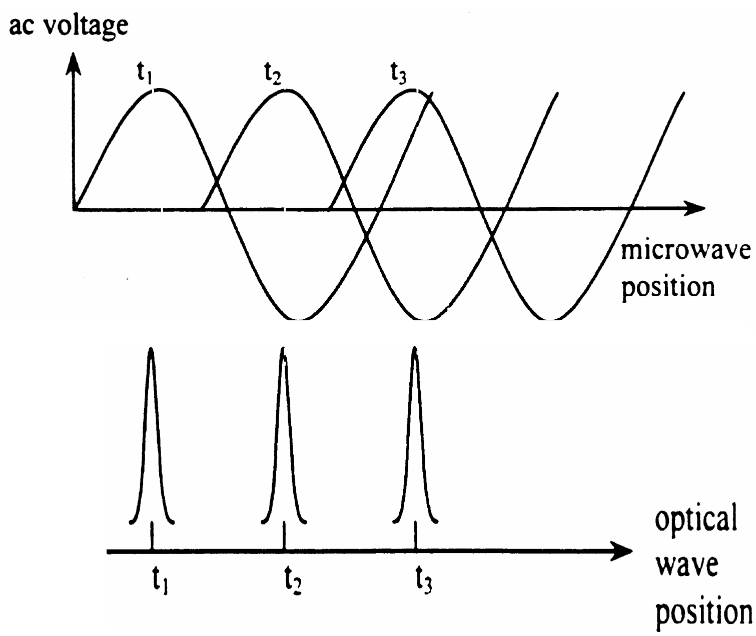

Fig. 4-13. Illustration of traveling wave.

Three important factors are the phase velocity difference between the optical wave and the rf –signal wave (velocity mismatch), the attenuation of the signal wave in transmission line and the characteristic impedance relation between modulator and the signal source (impedance mismatch). These are dependent upon the device configuration, namely the shape and size (thickness, width, length) of the electrode, the thickness of cladding layer in between the waveguide and electrode, and the material properties of electrode metal. Traveling wave electrode design can be analytically considered based on the Laplace equation for the electrostatic potential, which describes the microwave characteristics, namely

$$\varepsilon_x \frac{d^2\varphi}{dx^2} + \varepsilon_y \frac{d^2\varphi}{dy^2} = 0\,, \tag{4.14}$$

where φ is electrostatic potential, and ε_x and ε_y are the dielectric constants in the x and y directions. The effective dielectric constant [8] is then

$$\varepsilon_{eff.} = \frac{\varepsilon+1}{2} + \frac{\varepsilon-1}{2}(1+12\frac{h}{w})^{-1/2} - \frac{\varepsilon-1}{4.6}\frac{(t/h)}{(w/h)^{1/2}}\,, \tag{4.15}$$

and the characteristic impedance is

$$Z_{eff} = \frac{120\pi}{\sqrt{\varepsilon_{eff}}}\left[\frac{w'}{h} + 1.393 + 0.667\ln(\frac{w'}{h} + 1.444)\right]^{-1}, \tag{4.16}$$

where $$\frac{w'}{h} = \frac{w}{h} + \frac{1.25}{\pi}\frac{t}{h}(1 + \ln\frac{4\pi w}{t}), \tag{4.17}$$

w is the width, h is the thickness of electrode with bulk dielectric constant ε, and T is the thickness of upper cladding layer. The effective microwave refractive index is then

$$N_{eff} = \sqrt{\varepsilon_{eff}}\ . \tag{4.18}$$

Based on these equations, estimates of how the effective dielectric constant and characteristic impedance vary with electrode size may be obtained by Matlab calculations. From the calculation results, the effective dielectric constant increases with electrode width, but decreases with electrode thickness and cladding layer thickness. From Figure 4-4, the dielectric constants of PS-119 and CdSe at wavelengths larger than 1000 nm are 2.27 and 2.46, respectively. In order for electrodes to attain the same values, high conductivity metal Au (dielectric constant = 2.55) is chosen. Let the cladding layer thickness = 3 microns, so for a PS-119 film, the electrode width W and thickness h are 120-150 microns and 13-15 microns, respectively. For a CdSe film, electrode width W and thickness h are similarly 200-220 microns and 2-3 microns, respectively. These electrode sizes are quite different. From Figure 4-15, at those sizes, the impedances of the electrodes are low, only about 20 (PS-119) and 4 (CdSe) ohms, respectively. In most cases, the characteristic impedance should be 50 ohms, so other 30 (PS-119) and 46 (CdSe) ohm impedances should be added by other ways, such as by adding a resister in the circuit in order to meet the impedance matching condition.

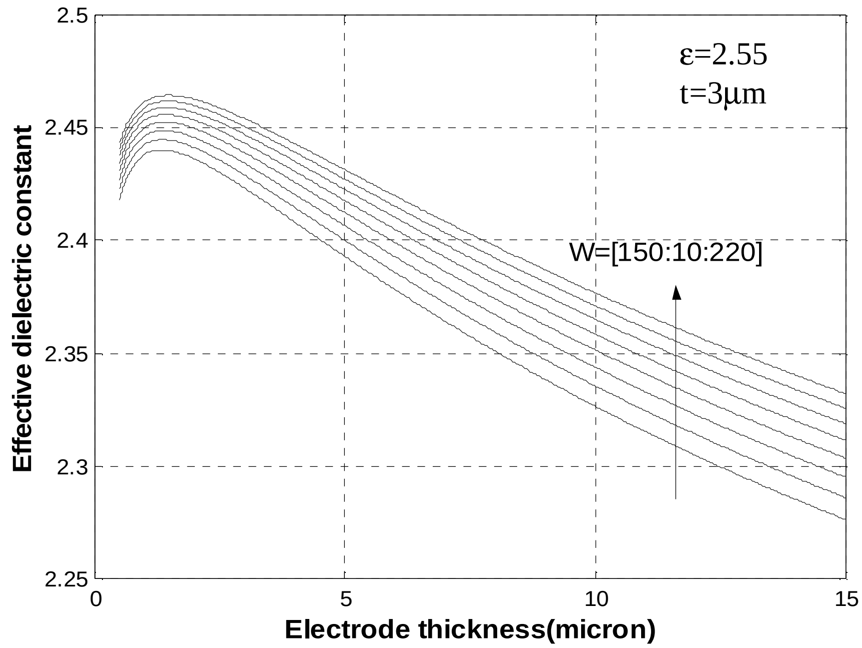

Fig. 4-14. Effective dielectric constant as a function of electrode size.

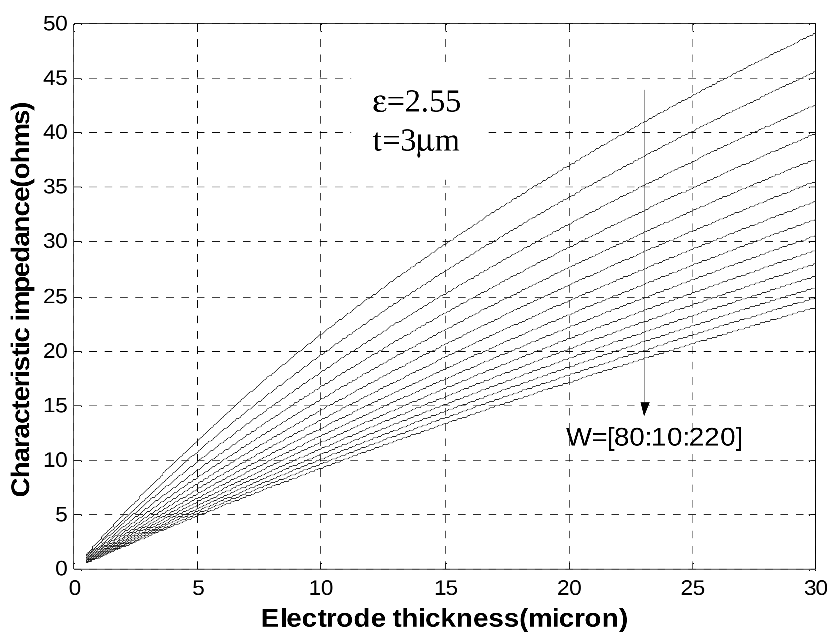

Fig. 4-15. Characteristic impedance as a function of electrode size.

All of the above calculations and designs are based on the effective refractive index method, which is simple, and straightforward, and reliable, particularly in defining the upper limits (close to the cutoff conditions) of the operation of devices [(3)]. For other aspects of design and device performance prediction, the beam propagation method (BPM) is preferred. It is more complicated, and more used in the industrial environment, and is beyond the scope of this.

4.4. Waveguide and electrode fabrication

In waveguide and electrode fabrication, many issues should be addresed. If the electro-optic polymer is coated on substrate by spin coating, the waveguide can be formed by selective poling. For ESA-formed electro-optic films, the waveguide should be formed by the photolithographic-etch process, which is the predominate process used to make optical channel waveguides. In this approach, photoresist is first spun onto electro-optic films, followed by bake, exposure, etch, and bake steps. The photoresist thickness is determined in accordance with waveguide mask design and etch selectivity. In determining the bake time and temperature, the thermal stability of the electro-optic films should be considered, and that the temperature can not be exceed the glass transition temperature Tg. Because the waveguide size (width) is larger than 1.5 microns, wet etching is feasible. This can reduce the cost significantly, although proper etchants should be used so that the electro-optic polymer is resistant to it. The cladding layer can be formed by the spin coating of polymers such as PMMA. Its thickness is controlled by its concentration and the coater spin RPM. The electrodes can be deposited by PVD technology such as DC sputtering or vacuum evaporation, but for high speed traveling electrodes, electroplating is better, because by carefully control the plating conditions (solution concentration, pH value, temperature and current/voltage), more condense, defect (mainly pore) free, electrodes can be formed.

In device performance tests, the bandwidth, half wave voltage, power consumption, losses, and output beam mode quality (mode size, single or multimode behavior) should be tested.

4.5. Conclusions

Based on the properties of electro-optic films, the applications of polymer and nano-cluster electro-optic films are discussed. The focus has been on the basic configurations and dimensions of MZI electro-optic intensity modulators. Dispersion curves of films (refractive index-wavelength relation) were measured, and the high frequency dielectric constants were calculated. Nano-cluster CdSe electro-optic film has a higher refractive index than the PS-119 polymer film, and these values they are much lower than that of semiconductor wafers such as Si, GaAs, and InP, but slightly higher than optical silica glasses. Accordingly optical silica glasses are the ideal substrates for those films, while semiconductor wafers are not useful. By analysis, the cutoff thickness was determined, which defines the minimum film thickness required for singlemode (m=0) light propagation; they are approximately 400 nm for CdSe film and 2500 nm for PS-119 film.

For channel waveguides, the effective refractive index varies as a function of the sizes of waveguide. The aspect ratio w/t, w, and t are determined versus the refractive index of the electro-optic films. We have consideral w/t=4.1 for PS-119 film, and w/t=1.1 for CdSe film. Modulator beam length and modulation index were discussed, for high speed operation. Modulator beam length should be carefully chosen to obtain high modulation index; similarly important is the refractive index match between core, substrate, and cladding layers.

For high speed operation, traveling wave electrode designs were considered, based on effective refractive index and impedance matching. The effective dielectric constant and characteristic impedance as a function of electrode configuration (sizes) were diagramed, and this served as a basic design suggestion for traveling wave electrodes.

4.6. References

1 G.R Mohlmann, Proc. of Fifth Tokyo Conf. Nonline. Opti. Mater..

2. Larry R. Dalton, et.al., J. Mater. Chem., 9, 1905(1999).

3. Hunsperger. Robert G: Photonic devices and systems. Marcel Dekker. Inc. 1994.

4. Blaine Johs, John A. Woollam, Craig M. Herzinger, et. al., Critical reviews of optical science and technology. CR72, 28(1999).

5. Ronald W. Waynant, Electro-optics handbook, 2nd ed, McGraw-Hill. 2000.

6. Govind P. Agrawal, Fiber-optic communication systems, 2nd ed., John Wiley & Sons, 1997

7. Amnon Yariv: Optical electronics in modern communications, 5th ed.. Oxford University Press. 1997.

8. I. Bahl and P. Bhartia, Microwave solid state circuit design. John Wiley & Sons, 1988.